networks of cords and tube-like structures were measured by Suite V3 (Leica).

For neuronal differentiation, each of MSCs at the 6-7 passage of culture 1.0×10^5 cells/dish had cultured on non-coated 35 mm dish in Neurosphere Progenitor Basal Medium (NPBM) (Lonza) with NP Maintenance Medium SingleQuots™ Kit (Lonza) (contains hEGF and hFGF) and NP Supplement SingleQuots™ Kit (Lonza) (contains NSF-1 and GA) as the addition factor for 11 days, designated for neurosphere formation. The average diameter of neurospheres was measured under an inverted microscope (Leica) using Suite V3 (Leica). The neurospheres were triturated using polished glass pipettes, and the obtained single-cell suspension had cultured in Gelatin-Coated 35 mm Dish (Iwaki, Shizuoka, Japan) in inducer medium. The medium was changed every 3 days. Expression of *neurofilament*, *neuromodulin* and *sodium channel, voltage-gated type I α* (*SCN1α*) mRNA was analyzed by real-time RT-PCR as described above at 25 days after cultivation. The primers were used as demonstrated previously [22,23]. Immunocytochemical analysis was also performed. The cells were fixed for 15 min in 4% paraformaldehyde in PBS at room temperature, reacted with mouse monoclonal neurofilament antibody (2F11) (Dako, Carpinteria, CA) (1: 100) for 1 h at room temperature, and followed by biotinylated anti-mouse IgG secondary antibody (Vector Laboratories, Burlingame, CA) for 30 min at room temperature. The cells were developed with the VECTASTAIN®Elite ABC reagent (Vector) and ImmPACT™ DAB Peroxidase Substrate (Vector).

Effect of the conditioned media

Each of MSCs at the 6-7 th passage of culture 60-70% confluence, the culture medium was switched to DMEM without serum, and the conditioned media (CM) were collected 24 h later and concentrated approximately 25-fold by an Amicon Ultra-15 Centrifugal Filter Unit with an Ultracel-3 membrane (Millipore, Billerica, MA). The protein concentration of the CM was determined by BradfordUltra™ (Expedeon, Cambridge, UK).

To assess the proliferative effect of the CM, NIH3T3 cells were seeded at 1×10^3 cells/well in a 96-well plate in DMEM supplemented with 5 μg/ml of the each CM without serum. Cell Counting Kit-8 was added to the 96-well plate, and the cell numbers were measured by Appliskan as described above. NIH3T3 cells (clone 5611) were purchased from Japanese Collection of Research Bioresources (JCRB) Cell Bank (Tokyo, Japan).

To examine the stimulatory effect of each CM on migratory activity of NIH3T3 cells, a horizontal chemotaxis assay was performed as described above.

The inductive potential of each CM into endothelial differentiation was assessed in the human umbilical vascular endothelial cell (HUVEC) line (7F3415) (Lonza). After HUVEC reached 60-70% confluence on 35 mm dish, the culture medium was switched to DMEM containing 2% FBS, 5μg/ml the conditioned medium from each of MSCs, 22.5 μg/ml heparin, 1 μg/ml ascorbic acid and 0.2 μg/ml hydrocortisone and had cultued for 11 days. Immunohistochemical staining was performed with mouse anti-Cadherin 5 (VE-Cadherin or CD144) (75) (BD biosciences) (1: 200) for 1h at room temperature and Alexa Fluor 488 goat anti-mouse IgG (H+L) secondary antibody (Life Technologies) (1: 200) for 1h at room temperature. The mean lengths of networks of cords and tube-like structures were measured by BZ-9000 analysis software (KEYENCE, Osaka, Japan) after counterstaining with 5 μg/ml Hoechst 33342 (Sigma-Aldrich).

The enhanced effect of each CM on neurite outgrowth was assessed in the human neuroblastoma cell line (TGW cells) (clone 0618) (JCRB Cell Bank). TGW cells were plated at 5.0×10^4 cells/ml on 35 mm dishes and were cultured in DMEM supplemented with 10% FBS for 24 h. Then, they were cultured supplemented with the each CM without serum for 12 h. For quantification of neurite outgrowth, the mean neurite length was measured by Suite V3 (Leica). At least, the neurite length of 100 cells was counted per sample.

To assess the immunomodulatory effect of the each CM, a mixed lymphocyte reaction (MLR) assay was performed as described previously [14]. Autologous peripheral blood mononuclear cells (PBMCs) and allogenic stimulator PBMCs from human were co-cultured at 1×10^5 cells per well in a 96-well plate in RPMI-1640 without arginine, leucine, lysine and phenol red (Sigma-Aldrich) supplemented with 5 μg/ml of the each CM. The cell numbers were measured using Cell Counting Kit-8 at 2, 12, 24 and 36 h as described above.

To assess the anti-apoptotic effect of the each CM, NIH3T3 cells were incubated with 500 nM staurosporine (Sigma-Aldrich) in DMEM supplemented with 5 μg/ml of the each CM for 3 h. The cells were harvested, treated with Annexin V-FLUOS Staining Kit (Roche Diagnostics) and analyzed by flow cytometry.

An experimental model of ectopic tooth transplantation model

An ectopic tooth transplantation model was used to evaluate regenerative potential. The porcine incisors were extracted, and their roots were cut out (6 mm in length, 1 mm in width). One end was sealed with zinc phosphate cement (GC, Tokyo, Japan). Each of MSCs (2×10^5 cells/100 μl at the 6-7 th passage of culture) was injected into the roots with collagen TE (Nitta Gelatin). Each of 4 roots with implanted MSCs was transplanted subcutaneously into 5-week-old severe combined immunodeficiency (SCID) mice (CB17; CLEA, Tokyo, Japan). Each root was harvested for histological and molecular biological analyses on day 21.

For histological analysis, all roots were fixed in 4% paraformaldehyde (Sigma-Aldrich) at 4°C overnight and embedded in paraffin wax (Sigma-Aldrich) after demineralization with Kalkitox™ (Wako, Osaka, Japan) at 4°C for a week. The paraffin sections (5 μm in thickness) were stained with hematoxylin and eosin (HE). Three sections at 150 μm intervals from a total 12 roots of each MSC transplantation were examined for relative amounts of regenerative tissue, as described previously [13]. To evaluate the cell densities, nuclear staining with 5 μg/ml Hoechst 33342 (Sigma-Aldrich) was performed.

For neovascularization analysis, immunostaining with rat monoclonal RECA1 antibody (HIS-52) (Monosan, San Diego, CA) (1: 200) for 1 h at room temperature and TEXIS RED® anti-rabbit IgG (H+L) secondary antibody (Vector Laboratories) (1: 200) for 1 h at room temperature were performed as described previously [13].

Table 1: Flow cytometric analysis of cell surface markers on mobilized MSCs (MDPSCs, MBMSCs and MADSCs) compared with each of colony-derived MSCs (DPSCs, BMSCs and ADSCs) at the 6-7th passage of culture. Data are expressed as the means ± SD of 3 determinations. The experiments were repeated three times (3 lots), and one representative experiment is presented.

		MDPSCs	DPSCs		MBMSCs	BMSCs		MADSCs	ADSCs
CD105		98.4±1.4	90.6±4.4		98.1±1.8	91.1±5.3		98.2±1.1	89.8±5.4
CXCR4	† **	14.1±1.1	5.1±1.1	**	12.0±1.2	2.7±0.9	**	11.7±1.2	3.6±1.1
G-CSFR	§ **	63.4±3.7	20.1±1.5	**	41.1±3.1	12.7±1.5	# ***	55.9±2.8	20.9±2.3

CXCR4, chemokine (C-X-C motif) receptor 4; G-CSFR, granulocyte colony-stimulating factor receptor.
(*$p < 0.05$, **$p < 0.01$, versus each colony-derived MSCs; †$p < 0.05$, versus MADSCs; §$p < 0.05$, versus MBMSCs; #$p < 0.05$, versus MBMSCs)

Table 2: Relative mRNA expression of stem cell markers, angiogenic and/or neurotrophic factors in mobilized MSCs (MDPSCs, MBMSCs and MADSCs) compared with corresponding colony-derived MSCs (DPSCs, BMSCs and ADSCs). The experiments were repeated three times (3 lots). Data are expressed as the means ± SD of 3 determinations.

	MDPSCs/DPSCs	MBMSCs/BMSCs	MADSCs/ADSCs
Sox2	* 4.3.±0.7	* 3.8±0.4	* 2.6±0.4
CXCR4	* 4.5±0.9	** 6.1±0.7	** 5.1±0.5
MMP3	* 4.5±0.7	* 3.8±0.7	* 3.2±0.6
VEGF	* 3.7±0.5	* 4.5±0.8	* 3.9±0.7
G-CSF	* 1.8±0.4	1.2±0.3	1.1±0.3
BDNF	* 4.7±0.6	* 4.5±0.7	** 7.0±0.7
GDNF	* 2.9±0.4	* 4.9±0.7	* 3.9±0.6
NPY	0.9±0.2	0.9±0.3	0.8±0.3

CXCR4, chemokine (C-X-C motif) receptor 4; MMP3, matrix metalloproteinase-3; VEGF, vascular endothelial growth factor ; G-CSF, granulocyte-colony stimulating factor; BDNF, brain-derived neurotrophic factor; GDNF, glial cell derived neurotrophic factor; NPY, Neuropeptide Y
(*$p < 0.05$, **$p < 0.01$, versus each colony-derived stem cells)

For molecular biological analysis, regenerated tissues were further isolated from each regenerated tissue at 21 days after transplantation. Total RNA was isolated and real-time RT-PCR amplifications were performed using markers for pulp tissue, *thyrotropin-releasing hormone degrading enzyme* (*TRH-DE*) [24] and *Syndecan3*, a marker for periodontal ligament, *periostin* and *periodontal ligament associated protein* (*PLAP*) as demonstrated previously [25]. The expression of these markers in the regenerated tissues was compared with that in normal pulp and periodontal ligament tissue from SCID mouse incisors.

To confirm that the regenerated tissue is functional pulp tissue, western blot analysis of the expression of TRH-DE was performed in each regenerated tissue at 21 days after transplantation as described previously [17]. Normal pulp tissue from the SCID mice incisors were used as a positive control. The anti-TRH-DE antibody (N-18) (1:1000) (sc-83177) (Santa Cruz Biotechnology Inc, CA) and anti-β-actin antibody (RB-9421) (Neo-Markers, Fremont, CA) were used. The protein bands were detected by ImmunoStar Zeta (Wako).

Statistical analyses

Data are expressed as means ± SD. *P* values were calculated using Student's *t* test and Tukey's multiple comparison test method in SPSS 21.0 (IBM, Armonk, NY).

Results

Isolation and characterization of mobilized MSCs

The morphology of the mobilized MSCs from all three tissue sources were stellate or spindle-shaped cells (Figure 1A). The mobilization efficiencies of mobilized MSCs, MDPSCs, MBMSCs and MADSCs were 17.5% ± 8.4, 8.4% ± 6.3 and 22.5% ± 6.3, respectively. MADSCs showed significantly higher mobilization efficiency compared with MBMSCs. The limiting dilution analysis of the 5 th passage culture showed that the frequencies of colony forming units (CFUs) in MDPSCs, MBMSCs and MADSCs were estimated to be 82.3% ± 2.8, 78.4% ± 1.5 and 75.8% ± 4.8, while those in DPSCs, BMSCs and ADSCs were 75.0% ± 3.8 , 72.0% ± 3.7 and 67.1% ± 1.6, respectively. The colony-forming units of MBMSCs and MADSCs were significantly higher than those of BMSCs and ADSCs, respectively.

Evaluation of the "stemness" of mobilized MSCs was performed by flow cytometric analysis in comparison with that of corresponding colony-derived MSCs (Table 1). Mobilized DPSCs have previously been characterized as the higher rate of CXCR4 and G-CSFR positive cells compared to colony-derived DPSCs [16,17]. In this study, the positive rates of CXCR4 and G-CSFR of mobilized MSCs were also significantly higher compared with those of colony-derived MSCs, respectively. There was no significant difference in the CD105 positive rate between mobilized and colony-derived MSCs. The positive rate of CXCR4 of MDPSCs was significantly higher than that of MADSCs and that of G-CSFR of MDPSCs and MADSCs were significantly higher than that of MBMSCs.

The mRNA expression of the stem cell markers (*Sox2, CXCR4*) and angiogenic and/or neurotrophic factors (*MMP3, VEGF, BDNF, GDNF*) were significantly higher in mobilized MSCs compared to corresponding colony-derived MSCs (Table 2).

The migratory activities of mobilized MSCs, particularly MADSCs, were significantly higher than those of colony-derived MSCs, respectively. MDPSCs and MADSCs showed the higher migratory activities than MBMSCs (Figure 1B).

The proliferation activities were significantly higher in mobilized

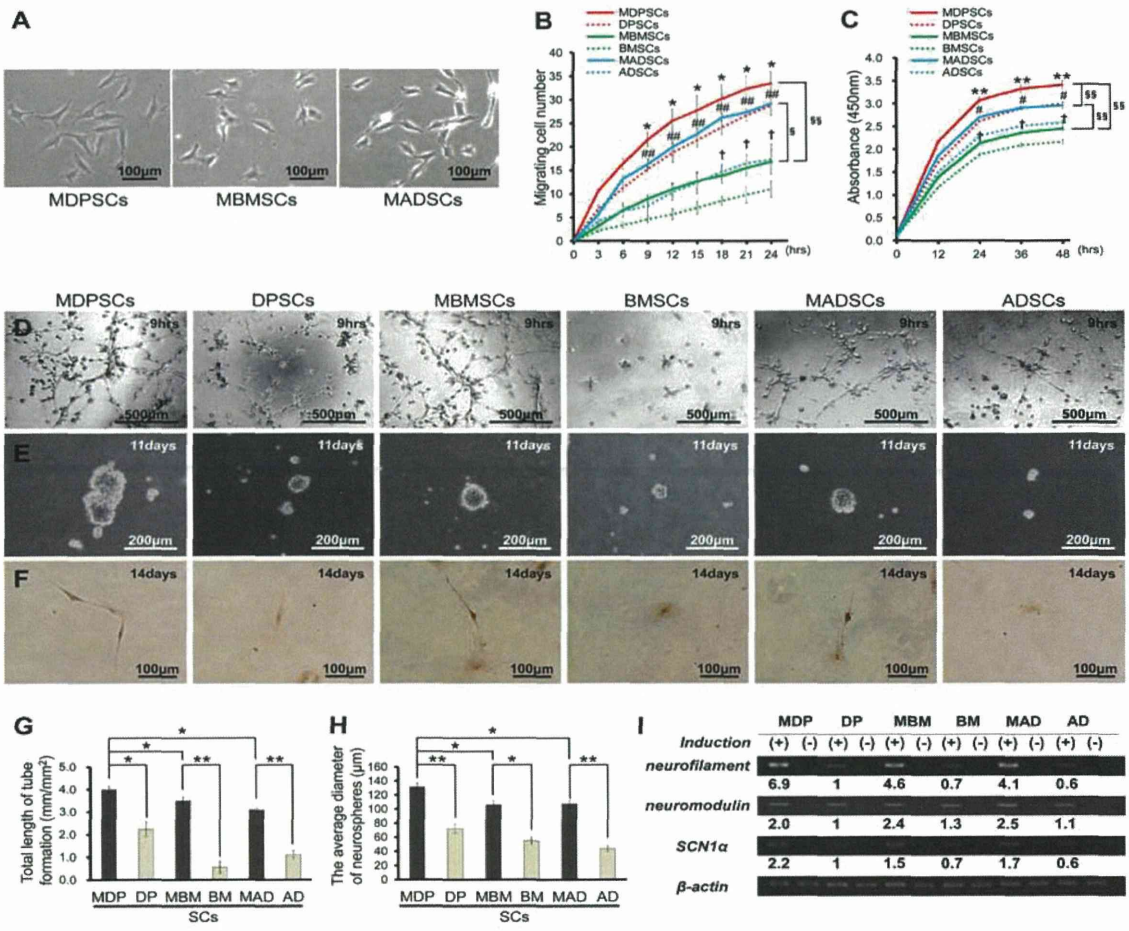

Figure 1: Properties of mobilized MSCs. (A) The mobilized MSCs at second passage of culture on day 2. (Mobilized dental pulp MSCs, MDPSCs; mobilized bone marrow-derived MSCs, MBMSCs; mobilized adipose-derived MSCs, MADSCs). (B) The migratory activity to G-CSF and (C) proliferation activity of each of MSCs (*$p < 0.05$, **$p < 0.01$, MDPSCs versus DPSCs; †$p < 0.05$, ‡$p < 0.01$, MBMSCs versus BMSCs; #$p < 0.05$, ##$p < 0.01$, MADSCs versus ADSCs; §$p < 0.05$, §§$p < 0.01$). (D) The endothelial differentiation assay using the matrigel after 9 h induction. (E) Neurosphere formation after 11 days induction. (F) Neurite outgrowth property after 14 days induction of dissociated neurosphere cells. (G) The mean lengths of networks of cords and tube-like structures (*$p < 0.05$, **$p < 0.01$). (H) The average diameter of neurospheres. (I) *Neurofilament, neuromodulin* and *sodium channel, voltage-gated type I α (SCN1α)* mRNA expression. The experiments were repeated three times (3 lots), and one representative experiment is presented. Data are expressed as the means ± SD of 3 determinations.

MSCs than in corresponding colony-derived MSCs. MDPSCs demonstrated the highest proliferation activity and MADSCs demonstrated the higher proliferation activity than MBMSCs (Figure 1C).

The differentiation potential of mobilized MSCs into endothelial cell lineage (Figure 1D) and neuronal cell lineage (Figure 1E and 1F) was compared with colony-derived MSCs, respectively. Total length of tube formation (Figure 1G) and the average diameter of neurospheres (Figure 1H) were significantly higher in mobilized MSCs compared to corresponding colony-derived MSCs. MDPSCs had the highest angiogenic and neurogenic potential among three mobilized MSCs. The mRNA expression of *neurofilament, neuromodulin* and *SCN1α* as neuronal markers demonstrated higher neurogenic potential of mobilized MSCs compared to colony-derived MSCs (Figure 1I).

These results demonstrated that not only DPSCs but also BMSCs and ADSCs contained subsets with high "stemness" can be isolated by G-CSF-induced mobilization.

Effect of the conditioned media

Next, the ability of the conditioned media (CM) of mobilized MSCs to accelerate cell proliferation and migration and suppress immunoreaction and apoptosis was investigated. The CM of mobilized MSCs was significantly more effective on the proliferation (Figure 2A) and migration (Figure 2B) in NIH3T3 cells than the CM of corresponding colony-derived MSCs. The CM of MDPSCs was the most effective on proliferation among the CM of three mobilized MSCs. The migratory effect of the CM of MDPSCs and MADSCs was higher than that of MBMSCs. A significantly enhanced immunosuppression by the CM of mobilized MSCs was shown by MLR assay compared to the CM of colony-derived MSCs, respectively (Figure 2C).

In the presence of each CM for 11days, HUVECs also formed extensive networks of cords and tube-like structures, typically associated with endothelial cells (Figure 2D). The CM of mobilized MSCs induced more dense formation of tube-like structures than the CM of corresponding colony-derived MSCs (Figure 2F). The CM of

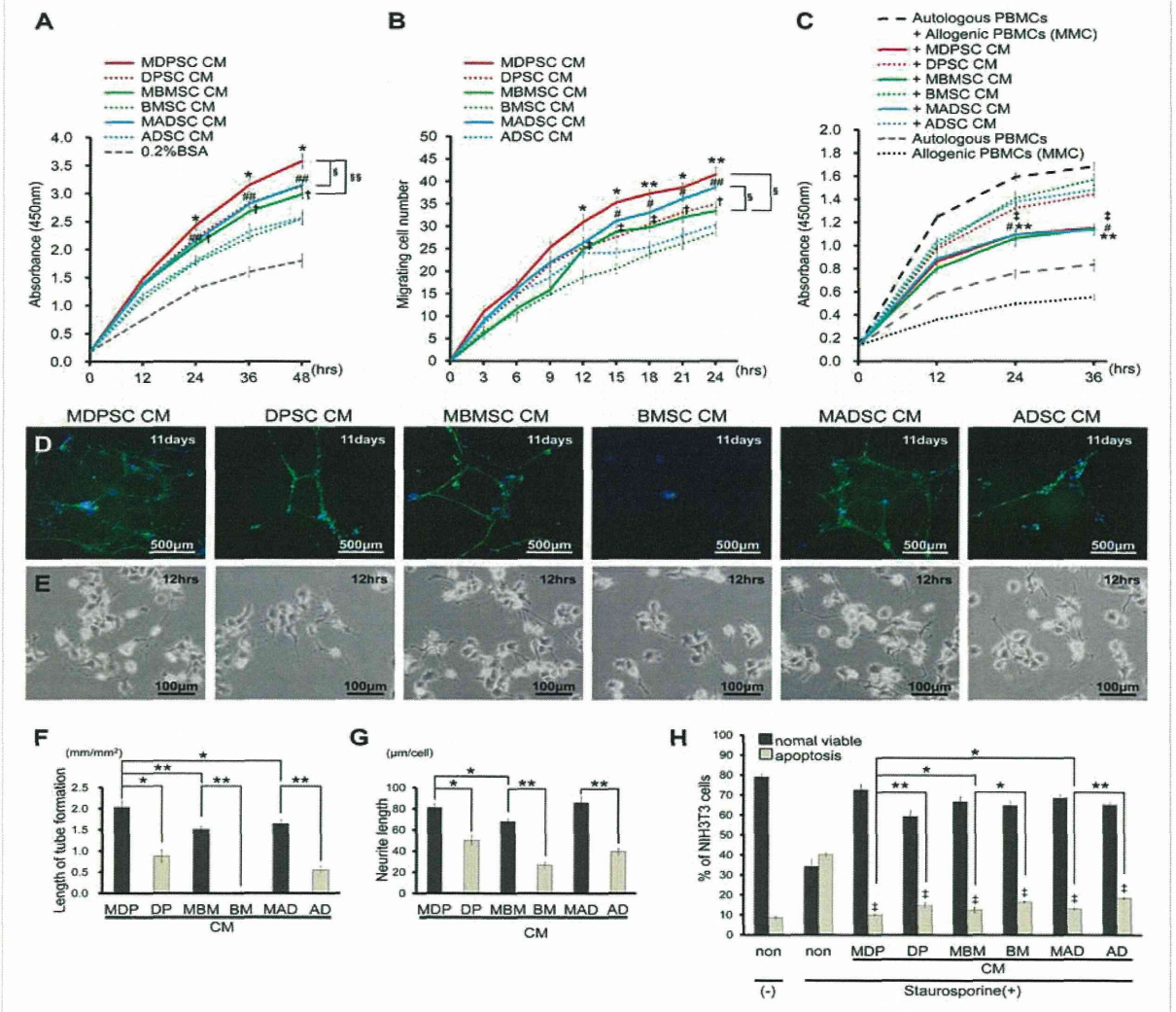

Figure 2: The effect of the conditioned media (CM) of each of MSCs *in vitro*. (A) Proliferation activity and (B) the migratory activity of NIH3T3 supplemented with the CM of MSCs (*$p < 0.05$, **$p < 0.01$, the CM of MDPSCs versus the CM of DPSCs; †$p < 0.05$, ‡$p < 0.01$, the CM of MBMSCs versus the CM of BMSCs; #$p < 0.05$, ##$p < 0.01$, the CM of MADSCs CM versus the CM of ADSCs; §$p < 0.05$, §§$p < 0.01$). (C) The mixed lymphocyte reaction (MLR) assay (MMC, treated with Mitomycin C; *$p < 0.05$, **$p < 0.01$, the CM of MDPSCs versus the CM of DPSCs; †$p < 0.05$, ‡$p < 0.01$, the CM of MBMSCs versus the CM of BMSCs; #$p < 0.05$, ##$p < 0.01$, the CM of MADSCs CM versus the CM of ADSCs; §$p < 0.05$, §§$p < 0.01$). (D) The endothelial differentiation assay of HUVECs for 11days on dish. Immunostaining with cadherin-5 (VE-cadherin) for vascular endothelial cells. (E) Neurite outgrowth in human neuroblastoma TGW cells enhanced by the CM of MSCs for 12 h. (F) Mean lengths of networks of cords and tube-like structures (*$p < 0.05$, **$p < 0.01$). (G) The mean length of neurite was compared (*$p < 0.05$, **$p < 0.01$). (H) The relative percentages of viable and apoptotic cells analyzed by flowcytometry (*$p < 0.05$, **$p < 0.01$; ‡$p < 0.01$, compared with staurosporine (+) and CM (-) apoptotic cells). The experiments were repeated three times (3 lots), and one representative experiment is presented. Data are expressed as the means ± SD of 3 determinations.

MDPSCs was most effective on endothelial differentiation among the CM of three mobilized MSCs. Neurite outgrowth in human neuroblastoma TGW cells was also enhanced by exposure to the CM of mobilized MSCs compared with the CM of corresponding colony-derived MSCs (Figure 2E and 2G). The CM of MDPSCs was significantly more effective on neurite outgrowth in TGW cells than the CM of MBMSCs. We also examined the anti-apoptotic effect of each CM. The survival rate of NIH3T3 cells was significantly enhanced by the CM of mobilized MSCs compared to the CM of corresponding colony-derived MSCs (Figure 2H). The CM of MDPSCs was the most effective on anti-apoptosis among the CM of three mobilized MSCs.

Thus, the CM of mobilized MSCs, especially the CM of MDPSCs, had superior trophic effects to the CM of corresponding colony-derived MSCs. These results demonstrated that the mobilized MSCs were isolated from bone marrow and adipose tissue by the G-CSF-induced mobilization as those isolated from dental pulp.

Pulp regenerative potential

To evaluate regenerative potential of mobilized MSCs, an ectopic tooth transplantation model was used. Pulp-like tissue with well-established vascularity was observed in all transplantations of mobilized MSCs on day 21 (Figures 3B, 3D, 3G). The total volume and the cell density of the regenerated tissue were much higher in the mobilized MSC transplantations compared to those in colony-derived MSC transplantations (Figures 3A, 3C, 3E, 3F), respectively. The MDPSC transplantation yielded the highest volume of regenerated tissue in all transplantations.

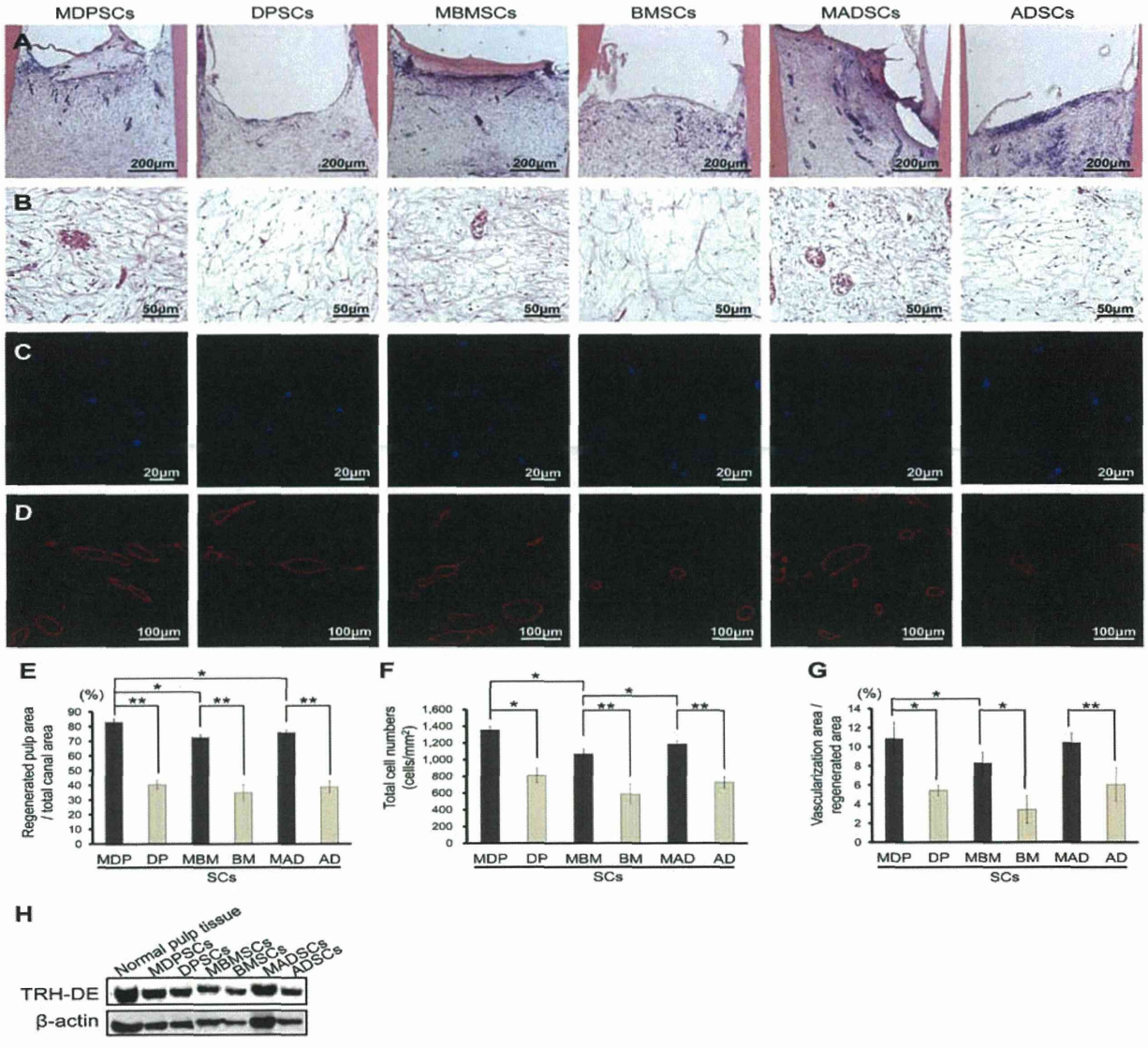

Figure 3: Regeneration of pulp tissue after ectopic tooth transplantation in severe combined immunodeficiency (SCID) mice subcutaneously. (A, B) Hematoxylin and Eosin. (C) Nuclear staining with Hoechst 33342. (D) Immunostaining with RECA1. (E) Ratio of regenerated area to root canal area (*$p < 0.05$, **$p < 0.01$). (F) The cell density in regenerated pulp tissues (*$p < 0.05$, **$p < 0.01$). (G) Ratio of neovascularization area to regenerated area (*$p < 0.05$, **$p < 0.01$). The experiments were repeated three times (3 lots), and one representative experiment is presented. Data are expressed as the means ± SD of 3 determinations. (H) Western blot analysis of the expression of TRH-DE, a pulp tissue biomarker, in each regenerated tissue.

Immunostaining with RECA1 demonstrated that neovascularization in the regenerated pulp tissue after transplantation of mobilized MSCs was significantly higher compared to corresponding colony-derived MSCs. The MDPSC transplantation induced the higher vasculature than the MBMSC transplantation (Figure 3D, 3G).

The regenerated tissue was further examined by real-time RT-PCR analysis and western blot analysis. The mRNA expression of *TRH-DE* and *syndecan 3*, biomarkers of pulp tissue, was higher in the mobilized MSC transplantations compared to that in corresponding colony-derived MSC transplantations and was similar to that in normal mouse pulp tissue. The expression of *periostin* was lower in the mobilized MSC transplantations compared to that in corresponding colony-derived MSC transplantations (Table 3). The protein expression of TRH-DE was almost in the same level in all transplantations (Figure 3H). These results demonstrated that pulp regenerative potential of the mobilized MSC transplantations was higher than that of corresponding colony-derived MSC transplantations.

Discussion

The G-CSF-induced stem cell mobilization method has previously been developed as an efficacious and safety method to isolate MSC subsets from dental pulp (MDPSCs) in canine and human [16,17]. MDPSCs represent following stem cell properties: higher ratio of CXCR4 and G-CSFR positive cells, higher proliferative and migratory activities, and higher trophic effects, including anti-

Table 3: Relative mRNA expression of tissue markers of pulp and periodontal ligament in regenerated tissue after stem cell transplantations. The experiments were repeated three times (3 lots). Data are expressed as the means ± SD of 3 determinations.

	MDPSCs	DPSCs	MBMSCs	BMSCs	MADSCs	ADSCs
TRH-DE	**1.3±0.3	0.6±0.1	*1.2±0.2	0.4±0.1	*1.2±0.2	0.5±0.2
Syndecan3	*0.9±0.2	0.4±0.1	*0.8±0.2	0.2±0.0	*0.9±0.2	0.3±0.1
Periostin	*0.1±0.0	0.3±0.1	**0.1±0.0	0.4±0.1	*0.1±0.0	0.3±0.1
PLAP	0.0±0.0	0.0±0.0	0.0±0.0	0.0±0.0	0.0±0.0	0.1±0.0

TRH-DE, Syndecan3: relative to mouse normal pulp tissue, *Periostin, PLAP*: relative to mouse normal periodontal ligament.
(*$p < 0.05$, **$p < 0.01$, versus each colony-derived MSC transplantation)

apoptosis, accelerating proliferation, migration, immunomodulation, angiogenesis and neuronal extension compared with colony-derived DPSCs. The present study has further demonstrated isolation of MSC subsets from bone marrow and adipose tissue of porcine mandible in the same individuals by the same method of G-CSF-induced mobilization of stem cells as MDPSCs. The flow cytometric analysis revealed the higher rate of CXCR4 and G-CSFR positive cells in MBMSCs and MADSCs as similarly demonstrated in MDPSCs compared with colony-derived MSCs, respectively. Each of mobilized MSCs of bone marrow and adipose tissue also indicated the higher migratory and proliferation abilities than corresponding colony-derived MSCs, which was similar to MDPSCs compared with DPSCs. These results suggested the utility of G-CSF-induced stem cell mobilization to isolate MSC subsets from other tissues including bone marrow and adipose tissue.

The present investigation has demonstrated that the regenerative potential of each of mobilized MSCs was higher than that of corresponding colony-derived MSCs in an experimental model of ectopic tooth transplantation in SCID mice. Growing evidence revealed that the beneficial effects of MSCs are predominantly caused by the multitude of bioactive molecules secreted by MSCs, the trophic factors [2]. Our previous studies have demonstrated that the endogenous cells from the surrounding tissue migrate and proliferate in the tooth root canal by trophic factors released from the transplanted pulp MSCs. These trophic factors also induce angiogenesis/neurogenesis and re-innervation *in vivo* [14,16,17]. Thus, the biological properties of the CM of mobilized MSCs were compared with the CM of corresponding colony-derived MSCs *in vitro*. The CM of mobilized MSCs enhanced proliferation and migratory activity, immunosuppression, angiogenic potential, neurite extension and anti-apoptosis compared to the CM of corresponding colony-derived MSCs. In addition, trophic factors including *MMP3, VEGF, GDNF* and *BDNF* mRNA were expressed higher in each of mobilized MSCs compared with those in colony-derived MSCs, respectively. VEGF is a major regulator of blood vessel formation and function [26], due to induction of endothelial cell proliferation, enhanced cell migration and anti-apoptosis [27]. MMP3 is known as an enhancer for proliferation, migration, and survival of HUVECs [28]. The activation of MMP3 expression can degrade CTGF in the VEGF-CTGF complex and release the angiogenic activity of VEGF [29]. Neurotrophic factors, such as BDNF or GDNF, encourage repair and, potentially, new growth of neurons [30]. In particular, neurite extension is mediated via GDNF and its receptor RET in TGW cells [31]. Thus, these results indicated the mechanism of high regenerative potential of mobilized MSCs compared to corresponding colony-derived MSCs.

In this study, the stem cell properties were further compared among three mobilized MSCs isolated by the same isolation and expansion method from the same individuals. In three mobilized MSCs, MDPSCs showed the highest proliferation activity, and the highest differentiation abilities into endothelial cells and neuronal cells. The trophic effect of CM on proliferation, angiogenesis and anti-apoptosis, and pulp regeneration ability *in vivo* were also the highest in MDPSCs. Furthermore, the higher expression ratio of G-CSFR, higher migratory ability, higher trophic effect of CM on migration and neurite extension, and the higher cell density and vasculature in regenerated pulp tissue were demonstrated in MDPSCs compared with MBMSCs. In comparison with MBMSCs, MADSCs indicated the higher expression ratio of G-CSFR, higher migratory and proliferation abilities and higher trophic effect of CM on migration, and the higher cell density in regenerated pulp tissue. The present results demonstrate that stemness and regenerative potential of mobilized MSCs are dependent on tissue origin [32], although G-CSF-induced stem cell mobilization is useful for many tissues to isolate MSC subsets.

We had previously isolated mobilized DPSCs in canine [16] and human [17]. In this study, stem cell properties were further examined in porcine by using the same isolation method as previously demonstrated. Since the cell size was larger in porcine compared with that in canine and human, cell number applied to the upper chambers was reduced to 1.5×10^4 cells/100 µl from 2.0×10^4 cells/100 µl. As the result, the mobilized porcine DPSCs indicated the similar cell properties to the others, suggesting that G-CSF-induced stem cell mobilization might apply to any type of cells across animal species by the same method.

Generally, a billion MSCs are needed to be administered for therapeutic efficacy, since only ~1% of the cells reach the ischemic myocardium after systemic infusion. The high migratory ability of mobilized MSCs due to high content of CXCR4 positive and G-CSFR positive cells may provide a clinically useful methods to improve the homing of MSCs to the ischemic regions such as myocardium and brain by the CXCR4/SDF-1 axis [33,34] and G-CSFR/GCSF system [35].

The high paracrine effects of mobilized MSCs can modulate the microenvironment of the diseased tissues so as to protect the injured cells, promote survival and activate any available endogenous repair mechanisms with high angiogenic/vasculogenic, neurogenic and regenerative potential. The extraordinary immunomodulatory properties of mobilized MSCs enable autologous and heterologous transplantation. Mobilized MSCs can be transplanted directly without genetic modification or pre-treatment, and are able to migrate to the tissue injury sites. There is no teratoma formation concern after

transplantation [16], and no moral objection or ethical controversies involved in their attainment. These advantageous properties heighten the clinical applicability of mobilized MSCs in a wide range of diseases.

Conclusions

Our data has demonstrated the utility of G-CSF-induced stem cell mobilization for isolation of BMSC and ADSC subsets as DPSC subsets. The advantage of the mobilized MSCs with enhanced stemness, trophic effects and regenerative potential may provide considerable promise in clinical cell therapy.

Competing Interests

The authors have declared that no competing interests exist.

Acknowledgements

We thank Mr. Masaaki Shimagaki from Toray Industry Inc. for supplying the chemically treated transmembrane. This work was supported by the Budget for promoting science and technology in Japan, which directly follows the policy of the Council for Science and Technology Policy (CSTP), chaired by the Prime Minister (M.N.), and the Research Grant for Longevity Sciences (23-10) from the Ministry of Health, Labour and Welfare (M.N.). The authors deny any conflicts of interest related to this study.

References

1. Satija NK, Singh VK, Verma YK, Gupta P, Sharma S, Afrin F, et al. Mesenchymal stem cell-based therapy: a new paradigm in regenerative medicine. J Cell Mol Med. 2009; 13: 4385-4402.
2. Bronckaers A, Hilkens P, Martens W, Gervois P, Ratajczak J, Struys T, et al. Mesenchymal stem/stromal cells as a pharmacological and therapeutic approach to accelerate angiogenesis. Pharmacol Ther. 2014; 143: 181-196.
3. Gimble JM, Katz AJ, Bunnell BA. Adipose-derived stem cells for regenerative medicine. Circ Res. 2007; 100: 1249-1260.
4. Ito K, Aoyama T, Fukiage K, Otsuka S, Furu M, Jin Y, et al. A novel method to isolate mesenchymal stem cells from bone marrow in a closed system using a device made by nonwoven fabric. Tissue Eng Part C Methods. 2009; 16: 81-91.
5. Lin K, Matsubara Y, Masuda Y, Togashi K, Ohno T, Tamura T, et al. Characterization of adipose tissue-derived cells isolated with the Celution™ system. Cytotherapy. 2008; 10: 417-426.
6. Semon JA, Maness C, Zhang X, Sharkey SA, Beuttler MM, Pandey AC, et al. Comparison of human adult stem cells from adipose tissue and bone marrow in the treatment of experimental autoimmune encephalomyelitis. Stem Cell Res Ther. 2014; 5: 2.
7. Stenderup K, Justesen J, Clausen C, Kassem M. Aging is associated with decreased maximal life span and accelerated senescence of bone marrow stromal cells. Bone. 2003; 33: 919-926.
8. Oñate B, Vilahur G, Ferrer-Lorente R, Ybarra J, Díez-Caballero A, Ballesta-López C, et al. The subcutaneous adipose tissue reservoir of functionally active stem cells is reduced in obese patients. FASEB J. 2012; 26: 4327-4336.
9. Madonna R, Renna FV, Cellini C, Cotellese R, Picardi N, Francomano F, et al. Age-dependent impairment of number and angiogenic potential of adipose tissue-derived progenitor cells. Eur J Clin Invest. 2011; 41: 126-133.
10. Corselli M, Crisan M, Murray IR, West CC, Scholes J, Codrea F, et al. Identification of perivascular mesenchymal stromal/stem cells by flow cytometry. Cytometry A. 2013; 83: 714-720.
11. Orlic D, Kajstura J, Chimenti S, Jakoniuk I, Anderson SM, Li B, et al. Bone marrow cells regenerate infarcted myocardium. Nature. 2001; 410: 701-705.
12. Gronthos S, Zannettino AC, Hay SJ, Shi S, Graves SE, Kortesidis A, et al. Molecular and cellular characterisation of highly purified stromal stem cells derived from human bone marrow. J Cell Sci. 2003; 116: 1827-1835.
13. Ishizaka R, Hayashi Y, Iohara K, Sugiyama M, Murakami M, Yamamoto T, et al. Stimulation of angiogenesis, neurogenesis and regeneration by side population cells from dental pulp. Biomaterials. 2013; 34: 1888-1897.
14. Iohara K, Imabayashi K, Ishizaka R, Watanabe A, Nabekura J, Ito M, et al. Complete pulp regeneration after pulpectomy by transplantation of CD105$^+$ stem cells with stromal cell-derived factor-1. Tissue Eng Part A. 2011; 17: 1911-1920.
15. Braakman E, Schuurhuis G, Preijers F, Voermans C, Theunissen K, Van Riet I, et al. Evaluation of 'out-of-specification'CliniMACS CD34-selection procedures of hematopoietic progenitor cell-apheresis products. Cytotherapy. 2008; 10: 83-89.
16. Iohara K, Murakami M, Takeuchi N, Osako Y, Ito M, Ishizaka R, et al. A novel combinatorial therapy with pulp stem cells and granulocyte colony-stimulating factor for total pulp regeneration. Stem Cells Transl Med. 2013; 2: 521-533.
17. Murakami M, Horibe H, Iohara K, Hayashi Y, Osako Y, Takei Y, et al. The use of granulocyte-colony stimulating factor induced mobilization for isolation of dental pulp stem cells with high regenerative potential. Biomaterials. 2013; 34: 9036-9047.
18. Ponte AL, Ribeiro-Fleury T, Chabot V, Gouilleux F, Langonné A, Hérault O, et al. Granulocyte-colony-stimulating factor stimulation of bone marrow mesenchymal stromal cells promotes CD34$^+$ cell migration via a matrix metalloproteinase-2-dependent mechanism. Stem Cells Dev. 2012; 21: 3162-3172.
19. Cheng Z, Liu X, Ou L, Zhou X, Liu Y, Jia X, et al. Mobilization of mesenchymal stem cells by granulocyte colony-stimulating factor in rats with acute myocardial infarction. Cardiovasc Drugs Ther. 2008; 22: 363-371.
20. Khan M, Manzoor S, Mohsin S, Khan SN, Ahmad FJ. IGF-1 and G-CSF complement each other in BMSC migration towards infarcted myocardium in a novel *in vitro* model. Cell Biol Int. 2009; 33: 650-657.
21. Nakashima M. Establishment of primary cultures of pulp cells from bovine permanent incisors. Arch Oral Biol. 1991; 36: 655-663.
22. Iohara K, Zheng L, Ito M, Tomokiyo A, Matsushita K, Nakashima M. Side population cells isolated from porcine dental pulp tissue with self-renewal and multipotency for dentinogenesis, chondrogenesis, adipogenesis, and neurogenesis. Stem Cells. 2006; 24: 2493-2503.
23. Iohara K, Zheng L, Wake H, Ito M, Nabekura J, Wakita H, et al. A novel stem cell source for vasculogenesis in ischemia: subfraction of side population cells from dental pulp. Stem Cells. 2008; 26: 2408-2418.
24. Yamamoto T, Murakami M, Ishizaka R, Iohara K, Kurita K, Nakashima M. Identification of thyrotropin-releasing hormone (TRH)-degrading enzyme as a biomarker for dental pulp tissue. Dentistry. 2012; 2: 1000114.
25. Ishizaka R, Iohara K, Murakami M, Fukuta O, Nakashima M. Regeneration of dental pulp following pulpectomy by fractionated stem/progenitor cells from bone marrow and adipose tissue. Biomaterials. 2012; 33: 2109-2118.
26. Gerhardt H, Golding M, Fruttiger M, Ruhrberg C, Lundkvist A, Abramsson A, et al. VEGF guides angiogenic sprouting utilizing endothelial tip cell filopodia. J Cell Biol. 2003; 161: 1163-1177.
27. Chavakis E, Dimmeler S. Regulation of endothelial cell survival and apoptosis during angiogenesis. Arterioscler Thromb Vasc Biol. 2002; 22: 887-893.
28. Zheng L, Amano K, Iohara K, Ito M, Imabayashi K, Into T, et al. Matrix metalloproteinase-3 accelerates wound healing following dental pulp injury. Am J Pathol. 2009; 175: 1905-1914.
29. Laurent M, Martinerie C, Thibout H, Hoffman M, Verrecchia F, Le Bouc Y, et al. NOVH increases MMP3 expression and cell migration in glioblastoma cells via a PDGFR-α-dependent mechanism. FASEB J. 2003; 17: 1919-1921.
30. Joyce N, Annett G, Wirthlin L, Olson S, Bauer G, Nolta JA. Mesenchymal stem cells for the treatment of neurodegenerative disease. Regen Med. 2010; 5: 933-946.

31. Uchida M, Enomoto A, Fukuda T, Kurokawa K, Maeda K, Kodama Y, et al. Dok-4 regulates GDNF-dependent neurite outgrowth through downstream activation of Rap1 and mitogen-activated protein kinase. J Cell Sci. 2006; 119: 3067-3077.

32. Yamada Y, Fujimoto A, Ito A, Yoshimi R, Ueda M. Cluster analysis and gene expression profiles: a cDNA microarray system-based comparison between human dental pulp stem cells (hDPSCs) and human mesenchymal stem cells (hMSCs) for tissue engineering cell therapy. Biomaterials. 2006; 27: 3766-3781.

33. Ghadge SK, Mühlstedt S, Özcelik C, Bader M. SDF-1α as a therapeutic stem cell homing factor in myocardial infarction. Pharmacol Ther. 2011; 129: 97-108.

34. Robin AM, Zhang ZG, Wang L, Zhang RL, Katakowski M, Zhang L, et al. Stromal cell-derived factor 1α mediates neural progenitor cell motility after focal cerebral ischemia. J Cereb Blood Flow Metab. 2005; 26: 125-134.

35. Solaroglu I, Jadhav V, Zhang JH. Neuroprotective effect of granulocyte-colony stimulating factor. Front Biosci. 2007; 12: 712-724.

Citation: Hirose Y, Murakami M, Hayashi Y, Osako Y, Yamamoto T, Gotoh M and Nakashima M. Augmentation of Regenerative Potential of Mesenchymal Stem Cells by Granulocyte-colony Stimulating Factor (G-CSF) Induced Mobilization. J Stem Cell Res Transplant. 2014;1(2): 10.